Article

Geminate Charge Recombination in Alternating Polyfluorene Copolymer/Fullerene Blends

Swati De, Torbjrn Pascher, Manisankar Maiti, Kim G. Jespersen, Tero Kesti, Fengling Zhang, Olle Ingans, Arkady Yartsev, and Villy Sundstrm

J. Am. Chem. Soc., **2007**, 129 (27), 8466-8472• DOI: 10.1021/ja068909q • Publication Date (Web): 14 June 2007

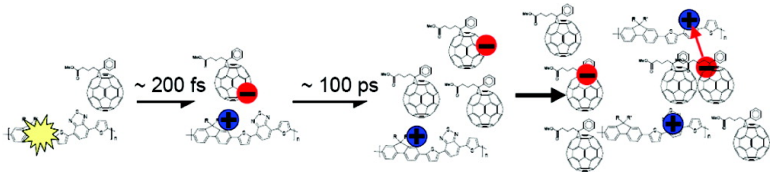

More About This Article

Additional resources and features associated with this article are available within the HTML version:

- Supporting Information
- Links to the 6 articles that cite this article, as of the time of this article download
- Access to high resolution figures
- Links to articles and content related to this article
- Copyright permission to reproduce figures and/or text from this article

View the Full Text HTML

J|A|C|S
ARTICLES
Published on Web 06/14/2007

Geminate Charge Recombination in Alternating Polyfluorene Copolymer/Fullerene Blends

Swati De,[†,§] Torbjörn Pascher,[†] Manisankar Maiti,[†] Kim G. Jespersen,[†] Tero Kesti,[†] Fengling Zhang,[‡] Olle Inganäs,[‡] Arkady Yartsev,[†] and Villy Sundström*[,†]

Contribution from Chemical Physics, Lund University, P.O. Box 124, SE-22100 Lund, Sweden, and Biomolecular and Organic Electronics, Department of Physics (IFM), Linköping University, SE-58183 Linköping, Sweden

Received December 13, 2006; E-mail: Villy.Sundstrom@chemphys.lu.se

Abstract: By measuring excited state and charge dynamics in blends of an alternating polyfluorene copolymer and fullerene derivative over nine orders in time and two orders in light intensity, we have monitored the light-induced processes from ultrafast charge photogeneration to much slower decay of charges by recombination. We find that at low light intensities relevant to solar cell operation relatively fast (~30 ns) geminate recombination is the dominating charge decay process, while nongeminate recombination has a negligible contribution. The conclusion of our work is that under solar illumination conditions geminate recombination of charges may be directly competing with efficient charge collection in polymer/fullerene solar cells.

Introduction

Conjugated polymer-based solar cells are promising alternatives to inorganic semiconductor photovoltaic devices.[1−3] Since the initial step in the photovoltaic action of polymeric solar cells is exciton dissociation leading to charge pairs, their performance has been found to improve considerably in the presence of an electron acceptor (e.g., a C_{60} derivative).[4,5] Early devices from this combination of materials gave low power conversion efficiencies because of low interfacial contact area between the donor and acceptor.[6] A major breakthrough in this direction was achieved by blending the polymer and a soluble fullerene derivative such that the two components form an interpenetrating network on the nanometer scale (the bulk heterojunction, BHJ).[7,8] Although this well-blended structure leads to reasonable external quantum efficiencies of ~50%, the large interfacial area present implies that there may be also heavy losses via electron−hole (e−h) recombination.[9−17] Thus, understanding the parameters influencing recombination dynamics in polymer/fullerene blends is a critical step toward optimizing device performance in future. This is the prime motivation for this work.

Charge carrier recombination in polymer/fullerene blends has been studied in the past by measuring the decay dynamics of charge carriers using a variety of time-resolved[9−19] and frequency domain techniques.[20] Sariciftci and co-workers have studied poly(phenylene vinylene) (PPV)/fullerene blends using nanosecond−millisecond transient absorption (TA) spectroscopy[11,12] and observed a biphasic decay of the signal: a fast (<20 ns) intensity-dependent decay and a slow (100 ns to 10 ms) intensity-independent decay. They assigned the fast decay to recombination of mobile PPV polarons and the slow decay to recombination of trapped polarons. Modeling of the slow decay measured in refs 11 and 12 led to the conclusion that although there is charge recombination (trap-limited), at the light intensities prevailing in operating solar cells, charge collection competes successfully with recombination.[9,10]

[†] Lund University.
[‡] Linköping University.
[§] On leave from the Department of Chemistry, University of Kalyani, Kalyani, Nadia 741235, India.

(1) Janssen, R. A. J.; Hummelen, J. C.; Saricifti, N. S. *MRS Bull.* **2005**, *30*, 33−36.
(2) Brabec, C. J. *Sol. Energy Mater. Sol. Cells* **2004**, *83*, 273−292.
(3) Nelson, J. *Curr. Opin. Solid State Mater. Sci.* **2002**, *6*, 87−95.
(4) Coakley, K. M.; McGehee, M. D. *Chem. Mater.* **2004**, *16*, 4533−4542.
(5) Sariciftci, N. S.; Smilowitz, L.; Heeger, A. J.; Wudl, F. *Science* **1992**, *258*, 1474−1476.
(6) Sariciftci, N. S.; Braun, D.; Zhang, C.; Srdanov, V. I.; Heeger, A. J.; Stucky, G.; Wudl, F. *Appl. Phys. Lett.* **1993**, *62*, 585−587.
(7) Yu, G.; Gao, J.; Hummelen, J. C.; Wudl, F.; Heeger, A. J. *Science* **1995**, *270*, 1789−1791.
(8) Brabec, C. J.; Zerza, G.; Cerullo, G.; De Silvestri, S.; Luzzati, S.; Hummelen, J. C.; Sariciftci, S. *Chem. Phys. Lett.* **2001**, *340*, 232−236.
(9) Nelson, J.; Choulis, S. A.; Durrant, J. R. *Thin Solid Films* **2004**, *451−452*, 508−514.
(10) Nelson, J. *Phys. Rev. B* **1999**, *59*, 15374−15380.
(11) Nogueira, A. F.; Montanari, I.; Nelson, J.; Durrant, J. R.; Winder, C.; Sariciftci, N. S. *J. Phys. Chem. B* **2003**, *107*, 1567−1573.
(12) Montanari, I.; Nogueira, A. F.; Nelson, J.; Durrant, J. R.; Winder, C.; Loi, M. A.; Sariciftci, N. S.; Brabec, C. *Appl. Phys. Lett.* **2002**, *81*, 3001−3003.
(13) Meskers, S. C. J.; van Hal, P. A.; Spiering, A. J. H.; Hummelen, J. C.; van der Meer, A. F. G.; Janssen, R. A. J. *Phys. Rev. B* **2000**, *61*, 9917−9920.
(14) Offermans, T.; Meskers, S. C. J.; Janssen, R. A. J. *Chem. Phys.* **2005**, *308*, 125−133.
(15) Offermans, T.; Meskers, S. C. J.; Janssen, R. A. J. *J. Chem. Phys.* **2003**, *119*, 10924−10929.
(16) Schultz, N. A.; Scharber, M. C.; Brabec, C. J.; Sariciftci, N. S. *Phys. Rev. B* **2001**, *64*, 245210.
(17) Savenije, T. J.; Kroeze, J. E.; Wienk, M. M.; Kroon, J. M.; Warman, J. M. *Phys. Rev. B* **2004**, *69*, 155205.
(18) Mozer, A. J.; Sariciftci, N. S.; Lutsen, L.; Vanderzande, D.; Österbacka, R.; Westerling, M.; Juska, G. *Appl. Phys. Lett.* **2005**, *86*, 112104.
(19) Mozer, A. J.; Dennler, G.; Sariciftci, N. S.; Westerling, M.; Pivrikas, A.; Österbacka, R.; Juska, G. *Phys. Rev. B* **2005**, *72*, 035217.
(20) Aarnio, H.; Westerling, M.; Österbacka, R.; Svensson, M.; Andersson, M. R.; Pascher, T.; Pan, J. X.; Sundström, V.; Stubb, H. *Synth. Met.* **2005**, *155*, 299−302.

10.1021/ja068909q CCC: $37.00

Offermans et al.[15] used transient resonant hole burning spectroscopy to study the charge recombination process in MDMO-PPV/PCBM films (where MDMO-PPV is poly[2-methoxy-5-(3′,7′-dimethyloctyloxy)-1,4-phenylene vinylene and PCBM is [6,6]-phenyl-C_{61}-butyric acid methyl ester); the measured intensity-independent hole decay dynamics coupled with Monte Carlo simulations[14] indicated that geminate recombination reduces the yield of holes within a few nanoseconds after excitation. Like Nelson et al.,[9,10] they also could fit their data by a power law, but the two groups differ in their interpretation of the recombination dynamics of MDMO-PPV/PCBM blends. According to the Nelson−Sariciftci groups, the recombination kinetics in solar cell blends is dominated by the slow decay arising from trapped charges, while the Janssen group suggests that recombination in these blends is dominated by the fast (<20 ns) component. Moreover, these groups also differ in their assignment of the fast component. Whereas Nelson−Sariciftci[9−12] ascribe it to intensity-dependent nongeminate-type recombination, Offermans et al.[14,15] assign it to intensity-independent geminate recombination. Meskers et al.[13] carried out time-resolved infrared studies on P3HT/fullerene blends (where P3HT is poly[3-hexylthiophene]) and showed that 80% of the charges created undergo geminate recombination within the first 30 ns after excitation, while the remaining survive for milliseconds.

Distinct fast (<20 ns) and slow (~150 ns) decay kinetics of microwave conductivity were also observed for MDMO-PPV/PCBM blends by Savenije et al.[17] The authors consider the observed decay of conductivity as recombination of free charge carriers, which, depending on the PCBM concentrations, can be either geminate or nongeminate.

Apart from recombination studies in polymer/fullerene blends, there have been experimental studies as well as simulations for devices.[21−24] The emerging picture here is also far from clear; both geminate and bimolecular recombination[23,24] as well as trapped charges[21,22] have been suggested to contribute to recombination. Thus, we see that there is no general consensus regarding the dynamics and mechanisms of charge recombination in polymer/fullerene blends, whether in bulk materials or in devices. Reasons for the different conclusions drawn from sometimes quite similar experiments is probably the different time resolution and excitation conditions (charge densities) used in the experiments. To monitor the full sequence of events, from charge formation to disappearance of charges (recombination), both high time resolution (femtosecond) and a wide time scale are required, and excitation intensities have to be varied over a sufficiently wide range to include both geminate and nongeminate recombination. In particular, achieving low intensities mimicking solar cell conditions is important.

To monitor the entire dynamics from the very early events immediately after photoexcitation to decay of charges, we performed transient absorption studies of APFO3/PCBM blends (where APFO3 is poly[2,7-(9,9-dioctylfluorene)-alt-5,5-(4′,7′-di-2-thienyl-2′,1′,3-benzothiadiazole)) using ultrashort femtosecond pulses combined with nanosecond flash photolysis, together covering over 9 orders in time, from ~30 fs to 50 μs. The intensity dependence of the recombination dynamics was also studied by covering 2 orders of magnitude in intensity, the lowest intensity being relevant for solar cell operational conditions. APFO3/PCBM blends have shown promise for solar cell applications.[25−29]

The major finding of our work is that light intensity-independent geminate recombination in APFO3/PCBM blends is quite fast (~30 ns). At high light intensities, recombination becomes even faster because of a contribution from intensity-dependent nongeminate recombination. This has important implications because geminate recombination is expected to prevail even under solar illumination conditions, implying that geminate recombination of charges may be directly competing with efficient charge collection in devices. We also conclude that, in blends, the polymer does not form an extended separated phase but is rather well mixed with PCBM.

Experimental Section

The samples were prepared following published procedures for synthesis of the active material of organic solar cells with previously reported performance.[30,31] In the present work, we are characterizing the light-induced processes in this material. APFO3 used in this study was synthesized according to ref 25 with a $M_n = 4900$, $M_W = 11\,800$, and a band gap of 2 eV. This polymer is widely used in polymer solar cells as an efficient photon absorber and electron donor[27,28] to the acceptor PCBM, which is a commercial product (Solenne, Groningen, The Netherlands). For preparing the samples with different PCBM loading, chloroform solutions with different stoichiometries of APFO3 and PCBM, 1:1, 1:3, and 1:4 by weight, were prepared by adding solvent to the mixtures. The solid films with a different amount of PCBM were deposited from the corresponding solutions by spin coating on clean glass substrates at 1000 rpm for 1 min.[32] To protect the films from further exposure to oxygen, they were covered by glass slides and sealed.

TA studies with 30-fs probe and pump pulses were performed as described previously.[27,28] Experiments were performed using both short (500-ps, 30-fs instrumental function) and long (20-ns, ~1-ps resolution) delay lines. Kinetics at even longer times were measured with a nanosecond TA (ns-TA) setup with 6-ns resolution, described in detail in ref 33. In these experiments, the samples were excited at 580 nm, and an unfocused helium−neon laser (543 nm) was used to probe the kinetics.

The kinetic modeling of the femtosecond data was performed using the Nelder−Mead Simplex method, and for the nanosecond data general linear regression was used.[34] To cover the time window of 30 fs to 50 μs, the three sets of data, femtosecond kinetics for both the short (500 ps) and long (20 ns) delay line and the nanosecond kinetics, were fitted simultaneously in a global fashion. Each femtosecond data set used for fitting covered the excitation intensity range 10^{13} to 10^{15} ph/cm^2

(21) Chirvase, D.; Parisi, J.; Hummelen, J. C.; Dyakonov, V. *Nanotechnology* **2004**, *15*, 1317−1323.
(22) Schilinsky, P.; Waldauf, C.; Brabec, C. J. *Appl. Phys. Lett.* **2002**, *81*, 3885−3887.
(23) Koster, L. J. A.; Smits, E. C. P.; Mihailetchi, V. D.; Blom, P. W. M. *Phys. Rev. B* **2005**, *72*, 085205.
(24) Mihailetchi, V. D.; Koster, L. J. A.; Hummelen, J. C.; Blom, P. W. M. *Phys. Rev. Lett.* **2004**, *93*, 216601.
(25) Inganäs, O.; Svensson, M.; Zhang, F.; Gadisa, A.; Persson, N. K.; Wang, X.; Andersson, M. R. *Appl. Phys. A* **2004**, *79*, 31−35.
(26) Andersson, L. M.; Inganäs, O. *Appl. Phys. Lett.* **2006**, *88*, 082103.
(27) Zhang, F. L.; Jespersen, K. G.; Björstrom, C.; Svensson, M.; Andersson, M. R.; Sundström, V.; Magnusson, K.; Moons, E.; Yartsev, A.; Inganäs, O. *Adv. Funct. Mater.* **2006**, *16*, 667−674.
(28) Jespersen, K. G.; Zhang, F.; Gadisa, A.; Sundström, V.; Yartsev, A.; Inganäs, O. *Org. Electron.* **2006**, *7*, 235−242.
(29) Lacic, S.; Inganäs, O. *J. Appl. Phys.* **2005**, *97*, 124901.
(30) Svensson, M.; Zhang, F. L.; Veenstra, S. C.; Verhees, W. J. H.; Hummelen, J. C.; Kroon, J. M.; Inganas, O.; Andersson, M. R. *Adv. Mater.* **2003**, *15*, 988−991.
(31) Svensson, M.; Zhang, F.; Inganas, O.; Andersson, M. R. *Synth. Met.* **2003**, *135*, 137−138.
(32) Yohannes, T.; Zhang, F.; Svensson, A.; Hummelen, J. C.; Andersson, M. R.; Inganas, O. *Thin Solid Films* **2004**, *449*, 152−157.
(33) Pascher, T. *Biochemistry* **2001**, *40*, 5812−5820.
(34) Beechem, J. M. *Methods Enzymol.* **1992**, *210*, 37−54.

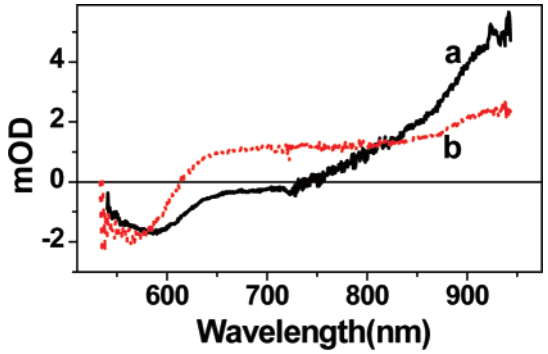

Figure 1. TA spectra at 10-ps pump−probe delay; pump = 580 nm, incident fluence = 1.2×10^{14} ph/cm^2 per pulse. (a) Neat APFO3 film. (b) 1:4 APFO3/PCBM blend.

per pulse, while only one nanosecond data set at low intensity was used. The data were weighted to put emphasis on the low-intensity traces, such that small relative errors in the high-intensity traces would not dominate the fit. Likewise, errors from the femtosecond part were given more weight than errors from the nanosecond part, so that noise in the early part of the nanosecond traces would not influence the fitted rates. The errors of the fitted parameters were estimated with *F*-statistics at a confidence limit of 99%.[34]

Results

The absorption spectrum of neat APFO3 film consists of two broad peaks centered at 384 and 540 nm that are assigned in ref 35. For the APFO3/PCBM blends with increasing concentration of PCBM, the absorbance at the peaks decreases and a distinct rise in absorbance due to PCBM is seen below 350 nm. The fluorescence emission spectra indicate significant quenching of the APFO3 fluorescence at 700 nm, in the presence of PCBM. The relative quantum yield of the 1:1 blend (APFO3/PCBM) with respect to neat APFO3 is 0.4%. This efficient quenching can occur only if there is direct quenching of the polymer excited states (i.e., there is no significant energy transfer between polymer segments before quenching). That this is the case is further supported by the fact that no time-resolved fluorescence could be observed with a streak camera setup having ~2 ps time resolution. For the neat polymer film, on the other hand, significant fluorescence was observed in the same setup and the fluorescence decay has a dominating component of ~50 ps. Using the fluorescence quantum yield in the blend and the lifetime component of 50 ps, we obtain 200 fs as the time scale (1/e) of the fast fluorescence quenching process in blends.

For transient absorption measurements, we used 580-nm pulses to excite the red wing of the low energy absorption band of APFO3. This ensures that there is negligible excitation of PCBM and also minimizes the effect of excited-state energy transfer in the polymer. The TA spectra in the region 500−1000 nm at 10 ps delay for the 1:4 APFO3/PCBM blend and the neat polymer at an incident photon flux of 1.2×10^{14} ph/cm^2 per pulse are shown in Figure 1. Three features are evident in the spectrum of the neat polymer: the ground-state bleach of the red band of the ground-state absorption located at 570 nm, the stimulated emission at 700 nm (where the steady-state fluorescence is observed), and a positive band at ~900 nm, the latter assigned mainly to the APFO3 excited state with only minor contribution from charge carriers.[28] This assignment of

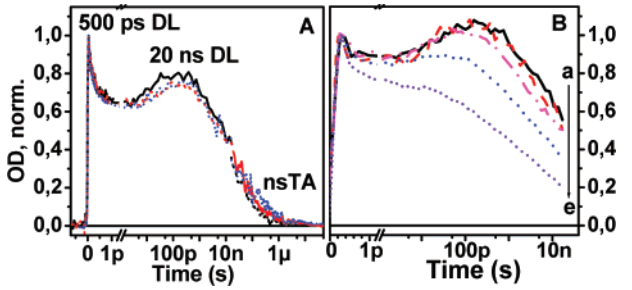

Figure 2. (A) TA kinetics over the entire time scale for different APFO3/PCBM blends at low fluence (~10^{13} ph/cm^2 per pulse): 1:1 blend − solid, black; 1:3 blend − dashed, red, and 1:4 blend − dotted, blue line. The nanosecond kinetics were smoothed and scaled, and the early parts of them were truncated for clarity of presentation. See real data points in Figure 3A. (B) Intensity dependence of the TA kinetics for the 1:1 blend at various incident photon fluences (ph/cm^2 per pulse): (a) 2.3×10^{13}, (b) 6.6×10^{13}, (c) 1.1×10^{14}, (d) 2.3×10^{14}, (e) 8.0×10^{14}. Note the scale: linear up to ~1 ps, log later on for both (A) and (B).

the ~900-nm band follows from the fact that TA kinetics of the neat polymer film probed at the bleach region (not shown) shows a recovery, which is identical to the TA decay observed when probing at 1000 nm. The transient spectrum of the APFO3/PCBM blend at 10-ps delay exhibits the polymer ground-state bleach, but lacks the stimulated emission and has a broad featureless absorption (650−950 nm) because of charged species only (see below).

Detailed information about the excited state and charge dynamics for the different APFO3/PCBM blends from 30 fs to 50 μs was obtained by combining the results of transient kinetics measured in three time windows: at 1000 nm, at 500 ps and 20 ns, and at 543 nm up to 50 μs (Figure 2A). In this way, the complete reaction sequence, from the initial excitation of the polymer to disappearance of the charges, was monitored in an unbroken chain of events. The kinetic traces for all three studied blends at low excitation flux (~10^{13} ph/cm^2 per pulse) show three main features: (i) an initial ultrafast decay (~200 fs) of the TA followed by (ii) a picosecond rise (~30 ps), and finally (iii) a second decay on the ~30-ns time scale.

Since charge carrier dynamics in polymer/fullerene-based devices has been shown to be dependent on the concentration of the carriers, we also examined the effect of incident light intensity on the TA dynamics in the blends. Figure 2B shows the intensity dependence of the kinetics for the 1:1 blend with the excitation intensity varied over almost 2 orders of magnitude. At the two lowest intensities ($<6.6 \times 10^{13}$ ph/cm^2 per pulse), the kinetics are intensity-independent within experimental error. We note that, at 20 ns, about 50% of the initial signal has decayed and very small amplitude extends into the microsecond time region. Above $\sim 1 \times 10^{14}$ ph/cm^2 per pulse, the kinetics becomes strongly intensity-dependent, with an increasingly faster decay at higher light intensities.

To evaluate the time scale of energy transfer in neat APFO3 films, we studied the intensity dependence of exciton−exciton annihilation (EEA). For other polymers, EEA dynamics has been observed to be a sensitive probe of energy transfer rate and transfer distance.[36] Within a simplified model, EEA for APFO3 can be described by an effective time-independent rate, $\gamma_{SS} = 2 \times 10^{-9}$ cm^3/s (data not shown), from which we can obtain

(35) Jespersen, K. G.; Beenken, W. J. D.; Zaushitsyn, Y.; Yartsev, A.; Andersson, M.; Pullerits, T.; Sundström, V. *J. Chem. Phys.* **2004**, *121*, 12613−12617.

(36) Stevens, M. A.; Silva, C.; Russell, D. M.; Friend, R. H. *Phys. Rev. B* **2001**, *63*, 165213.

Scheme 1. Processes Occurring after Light Absorption in APFO3/PCBM Blends[a]

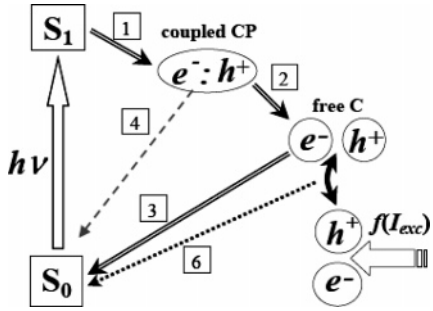

[a] 1: Charge photogeneration. 2: Free charge formation. 3: Free charge geminate recombination. 4: Recombination of Coulombically coupled charge pairs (shaded line indicates that this process is not significant in APFO3/PCBM). 6: Nongeminate recombination of free charges. Process 5 in the kinetic model, CP annihilation at high intensity, is not indicated.

the exciton diffusion coefficient (D_S) as $\gamma_{SS} = 8\pi D_S R_{SS}$,[36] where R_{SS} is the singlet−singlet interaction distance. Using the length of a chromophoric unit in APFO3 (∼1 nm) for R_{SS}, we get $D_S \approx 8 \times 10^{-4}$ cm^2 s^{-1}. The average exciton hopping time τ_h is then estimated to be ∼6 ps from the relation $R_{SS} = (2D_S\tau_h)^{1/2}$.[36]

A. Assignment of Processes. On the basis of our observation of strong fluorescence quenching in the blends, we assign the initial ultrafast (∼200 fs) decay observed in the TA dynamics to ultrafast charge transfer (CT) from the excited polymer to PCBM (process 1 in Scheme 1). This assignment is also in accordance with existing literature on other polymer/fullerene blends.[1−3,6−8] As a result of the charge transfer, a bound electron−hole pair is formed with the electron localized on PCBM and the hole on APFO3 (Scheme 1). The very short CT time implies that no unquenched excited state remains in the blend at times longer than ∼1 ps after excitation. Thus, at this time charges are the only photogenerated species present and responsible for the broad featureless absorption in the 650−950-nm range of the TA spectrum (Figure 1). The CT time of ∼200 fs in the blends is much faster than the excitation hopping time of ∼6 ps estimated for the neat polymer. Thus, the charge transfer in blends occurs before any excitation hopping can occur. This is only possible if next to every excited polymer segment there is a fullerene molecule. Therefore, we can conclude that there is no extended pure polymer phase present in these blends, and the polymer and fullerene form a homogeneous network on the nanometer scale.

The second decay that we observe on the nanosecond time scale is assigned to recombination of photogenerated charges. The long-time decay must arise because of decrease in charge population brought about by charge recombination. By decreasing the excitation intensity below ∼6×10^{13} ph/cm^2 per pulse, we find evidence of intensity-independent recombination dynamics (Figure 2B), implying first-order kinetics and thus a geminate character of the recombination (process 3 in Scheme 1). With increasing excitation intensity (>1×10^{14} ph/cm^2 per pulse), we observe a pronounced intensity dependence of the decay, a clear signature of nongeminate recombination (process 6 in Scheme 1)[27] and an unambiguous manifestation of free mobile charges (Figure 2B). Since geminate and nongeminate charge recombination occur on the same time scale (nanoseconds and longer) (at higher charge densities nongeminate recombination is even the faster process) and nongeminate recombination by its nature involves free mobile charges, geminate charge recombination also involves free charges.

Table 1. Results of Modeling

	blend 1:1		1:3	1:4
parameter	value	CI[a] 99%	value	value
$k_1 \times 10^{-12}$ [b]	5.3	4.8−5.8	4.9	4.5
$k_2 \times 10^{-10}$ [b]	3.4	2.7−4.4	2.4	2.1
$k_3 \times 10^{-7}$ [b]	3.4	3.1−3.8	3.0	2.9
σ_3[c]	7.3	6.0−9.1	7.5	5.8
$\gamma_{01} \times 10^{-13}$ [b,d]	6.6	3.9−7.3	26	18
α_1	0.23	0.02−0.49	0.88	0.59
$\gamma_{02} \times 10^{-11}$ [b,d]	4.6	3.1−6.1	8.7	7.8
α_2	1.06	0.98−1.17	1.17	1.11
$\epsilon_{singlet}$[e]	1.00	0.98−1.02	1.00	1.00
$\epsilon_{charge\ pair}$	0.63	0.62−0.64	0.65	0.67
ϵ_{charge}	0.81	0.80−0.83	0.82	0.82

[a] CI = confidence interval. [b] k_1, k_2, and k_3 are given in s^{-1}. γ_{01} and γ_{02} are given in M^{-1} s^{-1}. [c] σ_3 represents the factor in the rate constant k_3 corresponding to one σ in the log k_3 Gaussian distribution. [d] γ_{01} and γ_{02} are referenced at 1 ps and 1 ns. $\gamma_1(t) = \gamma_{01}/(t \times 10^{12})^{\alpha 1}$, $\gamma_2(t) = \gamma_{02}/(t \times 10^9)^{\alpha 2}$ with t in seconds. [e] $\epsilon_{singlet} = 7300 \pm 1400$ M^{-1} cm^{-1}; set to 1 in the model.

From the kinetics in Figure 2A, we see that after ultrafast formation of the Coulombically bound charge pairs (CPs) and before recombination of free charges, there is a rise of the TA signal on the picosecond time scale. It is therefore natural to associate this process, linking charge photogeneration and recombination, to formation of free charges (process 2 in Scheme 1). The internal quantum efficiency (IQE) of free charge formation useful for photocurrent production is directly related to the yield of free charges formed in competition with recombination of free charges (process 3) and recombination of Coulombically bound electron−hole pairs (process 4). Earlier, we showed that recombination of free charges is the process accounting for the nanosecond decay of charge concentration, but to what extent is recombination of Coulombically bound charge pairs contributing to the charge dynamics? By studying the dependence on PCBM concentration of the charge formation/recombination kinetics (Figure 2A and Table 1), we can get insight into this issue. We see that the rate of ultrafast (∼200 fs) charge generation (process 1) is independent of PCBM concentration; the rate of the reverse process, recombination of Coulombically bound charge pairs (process 4), therefore also must be independent of PCBM concentration. From the kinetics of Figure 2A, we see that the yield of free charges (the amplitude of the signal at ∼100 ps) is virtually independent of PCBM concentration, but the rate of the free charge formation changes by ∼40% in going from the 1:1 to the 1:4 blend. The only way to reconcile all these observations is that process 4, recombination of Coulombically coupled e−h pairs back to the ground state, is insignificant in APFO3/PCBM.

In summary, we observe three main processes in our TA kinetics at low intensity: charge pair generation, followed by formation of free charges, and finally intensity-independent recombination of free charges on longer time scales. At higher excitation intensities (>10^{14} ph/cm^2 per pulse), recombination becomes intensity-dependent because of a contribution from nongeminate recombination. At high light intensities, a charge pair annihilation process occurring on the few picoseconds time scale is also observed (section B). Unless efficient heterojunction solar cells based on other polymer/fullerene blends operate with qualitative different processes, we believe that this sequence of

Table 2. Summary of Processes Used in the Modeling of the Kinetics[a]

$S_0 + h\nu$	$\rightarrow S_1$		photoexcitation
1. S_1 + PCBM	$\rightarrow [e^-:h^+]$	k_1, first order	charge photogeneration
2. $[e^-:h^+]$	$\rightarrow e^- + h^+$	k_2, first order	free charge generation
3. $e^- + h^+$	$\rightarrow S_0$	k_3, first order	gem. recombination
4. $[e^-:h^+]$	$\rightarrow S_0$	not significant	e−h pair recombination
5. $[e^-:h^+] + [e^-:h^+]$	$\rightarrow S_0 + [e^-:h^+]$	γ_1, second order	charge pair recombination
6. $e^- + h^+$	$\rightarrow S_0$	γ_2, second order	nongem. recombination

[a] $[e^-:h^+]$ = Coulombically bound electron−hole pair; $e^- + h^+$ = free charges.

events is not unique for the studied APFO3/PCBM blend, but observed here as a result of our experimental ability to resolve all important steps in the sequence of light-induced processes of the material.

B. Kinetic Model for Charge Generation and Recombination in the Blends. On the basis of the processes of Scheme 1, we now discuss the kinetic model summarized in Table 2. We arrived at this model by globally fitting the low-intensity fs- and ns-TA kinetics for the 1:1 blend. Out of the three linear processes, 1 and 2 can be fit to single exponentials. Process 3 cannot be fit by a single exponential, neither with a pair of exponentials nor with a power law, but fits well using a Gaussian distribution in log k_3 space. Thus, the rate constant k_3 represents the mean value of this Gaussian distribution. The origin of the distributed rates may be a distribution either of electron-transfer activation energies or of electron-transfer distances. Our polymer/fullerene blends have been characterized as a disordered material for the longer time scale processes,[20] and therefore it is reasonable to expect that as a result of disorder a variation in both activation energy and distance contributes to the distribution in k_3.

To account for the intensity dependence of the recombination kinetics observed for intensities $>1 \times 10^{14}$ photons/cm^2 per pulse, the second-order processes 4 and 5 were added to the model. Process 5 represents the nongeminate recombination of charges, and process 4 is another second-order process that competes with formation of free charges. This process, reducing CPs formed upon exciton dissociation, we assign to charge recombination due to a CP−CP interaction. A similar phenomenon was observed by Savenije et al.[17] and assigned to a second-order process caused by an increased overlap of the Onsager spheres of the e−h pairs formed. Neither of the second-order processes could be fit by a time-independent rate, but required a time-dependent rate of the form $\gamma(t) = \gamma_0/t^{\alpha}$. A second-order process is typically coupled to mobility of reacting species; thus, this form of the rate for nongeminate recombination can be considered as a phenomenological representation of the time-dependent mobility of charge carriers.

The fits for the 1:1 blend are shown in Figure 3A. It can be seen that the above model provides a very good fit to our data, considering that we could simultaneously fit by the same model all the kinetic traces, covering 2 orders of magnitude in intensity (10^{13} to 10^{15} ph/cm^2 per pulse) and covering over 9 orders of magnitude in time (30 fs to 50 μs). Table 1 summarizes the fitting results. We obtain for the charge-transfer process $\tau \approx$ 200 fs, which agrees perfectly with our estimate based on the fluorescence quantum yield. The time constant of free charge formation is ∼30 ps, and the average geminate recombination time is ∼30 ns.

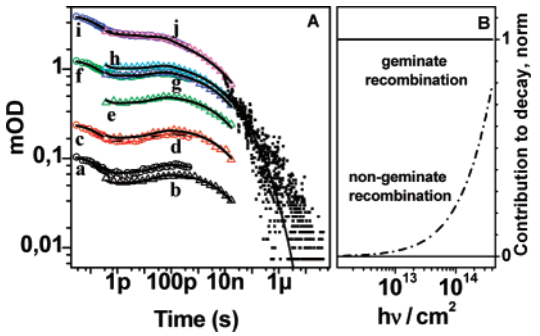

Figure 3. (A) TA kinetics for the 1:1 blend at various incident intensities fitted globally according to our model. Data points from pump−probe experiments with 500-ps and 20-ns delay line and from ns-TA experiment are shown by circles, triangles, and square dots, respectively. The solid lines are fits to the data. The fluences (ph/cm^2 per pulse) are (a) 1.5×10^{13}, (b) 1.0×10^{13}, (c) 3.0×10^{13}, (d) 3.0×10^{13}, (e) 7.6×10^{13}, (f) 1.5×10^{14}, (g) 1.5×10^{14}, (h) 1.8×10^{14}, (i) 4.9×10^{14}, (j) 4.8×10^{14}. (B) Contribution of nongeminate recombination of free charges relative to (normalized) geminate recombination to the overall charge decay kinetics for the 1:1 blend at different incident fluences.

As performance of APFO3/PCBM based solar cells is known to vary with different fullerene loading,[28] we also examined the effect of PCBM concentration on the TA dynamics of the blends. Referring to Figure 2A and Table 1, we note that the charge-transfer process is almost unaffected by a change in PCBM concentration, while formation of free charges and the recombination processes somewhat depend on PCBM concentration. Our model, thus far used for the 1:1 blend, also gave very good fits to the kinetics for the 1:3 and 1:4 blends (Table 1). In the 1:4 blend, the minor amplitude (∼3%) of the TA signal extending to long times (i.e., a few microseconds) could not be fit well by our model and has to be assigned to long-lived charges, possibly in deep traps, similar to the scenario suggested in ref 9. The observed dependence of the rates of free charge formation (∼40% change) and recombination (∼10% change) on PCBM concentration indicates some correlation with solar cell performance at different PCBM concentrations,[28] but the slowdown of geminate recombination is marginal compared to the rather drastic effect of PCBM concentration on solar cell performance. To obtain a better understanding of how and why the primary charge generation/recombination processes depend on material composition, we are presently extending these studies to a much wider polymer/PCBM concentration range and also to variations of morphology.

C. Our Results in Light of Existing Literature on Polymer/Fullerene Blends. We have observed ultrafast (∼200 fs) charge transfer from excited APFO3 to PCBM with efficiency of ∼100%. This result agrees well with previous work on other conjugated polymer/fullerene blends that has shown charge transfer with almost 100% efficiency provided the morphological demands are met.[1−3,6,7] In such samples, the initial electron transfer from the excited polymer to the fullerene acceptor occurs very rapidly and can be as fast as 45 fs.[8]

The key finding of our study is that, at low incident intensities ($<6 \times 10^{13}$ ph/cm^2 per pulse) following formation of free charges, we observe intensity-independent (geminate) recombination of charges. In neat conjugated polymers, geminate recombination has been previously reported to reduce the

photocurrent yield.[37] One picture that emerges from existing literature on polymer/fullerene blends is that recombination is nongeminate, occurring as a result of charge diffusion.[9−12,18,19] This is manifested by the dependence of the recombination rate on charge mobility,[18,19] charge trapping,[11,12] charge density,[11,12] and temperature.[10] The other view, that recombination is mainly of geminate nature, is supported by the reports.[13−15,38−40] In the present study, by analyzing the variation of the fully time-resolved recombination dynamics over 2 orders of magnitude in intensity, we can distinguish the conditions where geminate and nongeminate charge recombination prevail. Figure 3B shows the relative contribution of the geminate and nongeminate recombination as a function of incident intensity. We note that, only at intensities $\geq 10^{14}$ ph/cm^2 per pulse (corresponding to charge densities of $\sim 8 \times 10^{18}$ charges/cm^3), nongeminate recombination starts to contribute significantly.

It must be noted that geminate recombination in our case (Scheme 1) is not recombination of the initially formed Coulombically bound e−h pair, as is commonly understood in the Onsager picture.[13−15,39,40] In such a case, it is assumed that, for geminate recombination, there is a strong competition between charge separation and geminate recombination of the initially formed e−h pair, and such geminate recombination is fast enough to compete with charge separation.[39] Geminate recombination in our case differs in that it is preceded by formation of free charges, and thus it is the free charges that participate in geminate recombination. This process is observed when the concentration of free charge carriers is too low for a nongeminate recombination to occur, and the only charge an electron may recombine with is its own hole, resulting in geminate type of recombination.

Using the microwave conductivity method for MDMO-PPV/PCBM blends with different PCBM concentrations, Savenije et al.[17] suggested geminate recombination of free holes at low concentration of PCBM and nongeminate recombination of free electrons at high PCBM concentration. Apparently, the same character of recombination has to be observed for both electron and holes as they recombine with each other. In the microwave conductivity measurements, it is the carriers of the highest mobility that dominate the signal even if these carriers are in the minority. In the experiments reported in ref 17, at low PCBM concentration the acceptor molecules were considered to be separated from each other by the polymer leading to domination of hole conductivity in the signal. At high concentration, when PCBM-rich aggregates were formed, the signal was dominated by electron conductivity in this phase of the blends. Though the microwave conductivity method is a very sensitive technique, its restricted temporal resolution and spatial limitations (∼18 ns and ∼5 nm, respectively)[17] complicate direct comparison with our results.

As a rise of TA, we observe another process that occurs after charge generation and before charge recombination. We have assigned this process to charge separation (i.e., breaking of the electron and hole pair held together by the mutual Coulomb attraction) and formation of free charges. Conversion of coupled charge pairs to separated charges is often considered not to be accompanied by spectral changes in the visible part of the spectrum. However, Vardeny et al. have shown that the spectral signatures of polaron pairs and isolated polarons are different for several polymers.[41] The broad spectral coverage in the present work and our ability to record weak TA signal dynamics, free of nongeminate recombination, made it possible to distinguish the conversion of bound charge pairs into separated charges.

The rate of nongeminate recombination is determined by the mobility of free charges. Therefore, the time dependence of the nongeminate recombination rate that is used in our model reflects a decrease of the charge carrier mobility with time. Observation of a similar time-dependent charge mobility decrease has been reported by Juska et al.[18,19] for MDMO-PPV/PCBM blends.

D. Relevance to Devices. It is important to examine the relevance of the present results in relation to solar cell performance under solar intensities. At the ASTM standard for solar testing, AM 1.5 (100 mW/cm^2), the photon flux obtained in 30 ns (corresponding to the 1/e time for geminate recombination that we obtain) is $\sim 1 \times 10^{10}$ ph/cm^2 per pulse. At the lowest intensities used in our experiments (1×10^{13} ph/cm^2 per pulse), the photon flux is 1000 times higher than solar illumination. From Figure 3B, it can be seen that, under solar illumination conditions, nongeminate recombination would hardly contribute to the charge carrier decay dynamics in our blends. Since geminate recombination is insensitive to light intensity and concentration of charges, it must be considered as an important factor controlling the charge decay dynamics in APFO3/PCBM blends also under solar irradiation. Although we concluded that nongeminate recombination has little impact on the charge decay dynamics at solar intensities in a material study, it is somewhat less straightforward to determine the relevance of the concentration-dependent nongeminate recombination for solar cell performance. The concentration of charges in a functional solar cell is not a constant value throughout a cell[23,29] and depends on whether a short or open circuit is considered. In both cases though, through most of the solar cell thickness the charge concentration is less or much less than 10^{17} cm^{-3},[23] which corresponds to a light flux of 2×10^{12} ph/cm^2 per pulse in our case. From Figure 3B, one can see that nongeminate recombination contributes negligibly to the charge decay and therefore should not be a major factor of recombination in solar cells neither.

Our work on APFO3/PCBM blends shows that photogeneration of charges occurs with ∼100% efficiency while it is known that IQEs of the best performing device (with a 1:4 blend as the active layer) reach 68% at the low energy absorption maximum of APFO3.[42] This suggests that there are recombination losses within the device that prevent more efficient charge collection. Often in literature on polymer/fullerene-based solar cells, one comes across the extraction time of ~ 1 μs. At first glance, it appears then that recombination (geminate) is too fast for efficient charge extraction. However, the fact that charges can be efficiently extracted from solar cells indicates that a 1-μs extraction time is not the relevant comparison with the geminate

(37) Muller, J. G.; Lemmer, U.; Feldmann, J.; Scherf, U. *Phys. Rev. Lett.* **2002**, *88*, 147401.
(38) Muller, J. G.; Lupton, J. M.; Feldmann, J.; Lemmer, U.; Scharber, M. C.; Sariciftci, N. S.; Brabec, C. J.; Scherf, U. *Phys. Rev. B* **2005**, *72*, 195208.
(39) Onsager, L. *Phys. Rev.* **1938**, *54*, 554−557.
(40) Bässler, H. *Primary Photoexcitations in Conjugated Polymers: Molecular Exciton versus Semiconductor Band Model*; Sariciftci, N. S., Ed.; World Scientific: Singapore, 1997.
(41) Lane, P. A.; Wei, X.; Vardeny, Z. V. *Phys. Rev. B* **1997**, *56*, 4626−4637.
(42) Persson, N. K.; Arwin, H.; Inganäs, O. *J. Appl. Phys.* **2005**, *97*, 034503.

recombination time. One must keep in mind that in real-life solar cell devices, the electric field affects the light-induced processes, and there is charge migration under the influence of a local electric field inside the photoactive material. The time (t) for charge migration under a potential (V) through a distance l is given by $t = l^2/\mu V$, where μ is the mobility of the charge carrier.[43,44] Using this expression, we estimated that, under a typical potential of 1 V,[14] an electron mobility of 10^{-3} cm^2 V^{-1} s^{-1},[43,44] and an IQE of 50%, the ~30-ns recombination time translates to an effective recombination distance of ~30 nm, comparable to the morphological structures seen in APFO3/PCBM blends.[27] This suggests that optimization of solar cell morphology is important for reduction of recombination as well as for improving charge transport.

Conclusions

We have studied geminate and nongeminate charge recombination in APFO3/PCBM blends and conclude that geminate recombination is essential for solar cell performance, whereas nongeminate recombination is of little importance. Our results suggest that manipulation of the nanomorphology of polymer/fullerene blends may provide the solution to minimizing geminate recombination. The losses due to recombination could perhaps also be overcome if charge carrier mobility can be enhanced.

Acknowledgment. S.D. acknowledges the Department of Science and Technology, Govt. of India, for support in the form of the BOYSCAST program. The studies were supported by the Center of Organic Electronics, funded by the Swedish Strategic Research Foundation (SSF). Support was also obtained from the Swedish Research Council, the Swedish Energy Agency, the Knut&Allice Wallenberg Foundation, and the Crafoord Foundation. We thank Prof. Mats Andersson and his group at Chalmers University for polymer samples.

JA068909Q

(43) Tuladhar, S. M.; Poplavskyy, D.; Choulis, S. A.; Durrant, J. R.; Bradley, D. D. C.; Nelson, J. *Adv. Funct. Mater.* **2005**, *15*, 1171−1182.
(44) Mihailetchi, V. D.; van Duren, J. K. J.; Blom, P. W. M.; Hummelen, J. C.; Janssen, R. A. J.; Kroon, J. M.; Rispens, M. T.; Verhees, W. J. H.; Wienk, M. M. *Adv. Funct. Mater.* **2003**, *13*, 43−46.